

# ACCELERATION OF POSITRONS BY ELECTRON BEAM-DRIVEN WAKEFIELDS IN A PLASMA\*

K. V. Lotov, Budker INP, 630090, Novosibirsk, Russia

## Abstract

Plasma wakefield acceleration of positron beams in the wake of a dense electron beam (in the blowout regime) is numerically analyzed. The acceleration is possible only if the energy content of the wakefield is not very high. This contrasts with electron acceleration, for which the optimum performance requires as high driver currents and wave energies as possible. The positron beam must be placed between the first and the second bubble, in the region of increased density of plasma electrons. The efficiency of plasma-to-witness energy exchange can amount to several tens percent, but high efficiencies require precise location of the positron beam and sophisticated beam shapes. Unlike an electron witness, the positrons always get an energy spread of about several percent caused by the transverse inhomogeneity of the accelerating field.

## INTRODUCTION

Plasmas can sustain electric fields that are many orders of magnitude higher than those in conventional accelerating structures. This property is used in plasma wakefield accelerators (PWFA), in which one particle beam drives the high amplitude field in the plasma, and another beam (witness) is accelerated by this field. For collider applications of PWFA, it is desirable to succeed in acceleration of both electrons and positrons in the plasma. Up to now, studies of positron acceleration were mainly related to Stanford experiments [1] and the afterburner concept [2] and as yet limited to positron-driven waves [3]. Positrons, however, are rather “expensive” particles to be used as a driver in other conceivable applications of PWFA, so it is important to analyze the possibility of positron acceleration in the wake of an electron beam.

In the linear regime, there is no principal difference in behavior of electrons and positrons. The difference appears at higher beam densities and nonlinear plasma responses. If the density of the electron driver is greater than the plasma density, then PWFA switches to the so-called blowout regime [4]. In this regime, all plasma electrons are ejected off the beam propagation channel, and an electron-free region (bubble) is formed around the drive beam. In the case of electron acceleration, the blowout regime offers several advantages over the linear regime [4, 5], so we check the option of positron acceleration in the blowout wake of a dense electron beam.

All simulations presented are made with two-dimensional code LCODE [6, 7] in the axisymmetric

geometry  $(r, \varphi, z)$  with the  $\vec{z}$ -axis being the direction of beam propagation. For characterization of beam-plasma energy exchange and wakefield energy content, we use the dimensionless energy flux in the co-moving window [8]:

$$\tilde{\Psi} = \frac{4\pi e^2}{m^2 c^5} \int_0^\infty \left( \frac{c}{8\pi} ((E_r - B_\varphi)^2 + E_z^2) + \sum_{\text{u.v.}} (\gamma - 1) m c^2 (c - v_z) \right) 2\pi r dr, \quad (1)$$

where the summation is carried out over plasma electrons in the unit volume,  $\gamma$  is the relativistic factor of plasma electrons,  $v_z$  is their longitudinal velocity, and other notation is common. Focusing properties of the wave are conveniently illustrated by maps of the dimensionless potential  $\tilde{\Phi}$ , derivatives of which show the force exerted on axially propagating ultrarelativistic positron:

$$\frac{\partial \tilde{\Phi}}{\partial z} = -\frac{\omega_p}{c E_0} E_z, \quad \frac{\partial \tilde{\Phi}}{\partial r} = -\frac{\omega_p}{c E_0} (E_r - B_\varphi), \quad (2)$$

where  $\omega_p = \sqrt{4\pi n_0 e^2/m}$  is the plasma frequency,  $E_0 = mc\omega_p/e$ , and  $n_0$  is the unperturbed plasma density.

## TRANSVERSE EQUILIBRIUM AND BEAM LOADING

The first problem specific to positrons is related to the transverse equilibrium. As the energy content of the plasma wave increases, the region of favorable (inward) focusing force for positrons shrinks. In the blowout regime, in the limit of  $\tilde{\Psi} \gg 1$  the length of this region tends to zero (Fig. 1a,c). When initially placed on axis in the accelerating field at the head of the second bubble, positrons shift radially and take up an off-axis position (Fig. 1c), resulting in a drastic growth of the beam emittance.

There are, at least, two ways to improve the transverse field structure in the blowout regime. The first one is to make an ion-free channel on axis. With no ions, there is no source of the transverse force near the bubble axis, and positrons stay in indifferent equilibrium. Another way is to operate at moderate energy contents of the plasma wave. In this case, there exists a lengthy interval of high electron density between the first and the second bubble (Fig.2a). The potential well in this interval has the minimum on axis (Fig.2c), which means the favorable focusing.

The second problem is related to the slope of the accelerating field. A dense witness always reduces the field as compared to the unloaded case (Fig.2b). If the derivative  $\partial|E_z|/\partial z$  is positive even in the unloaded case, then the witness augments it further, and zero energy spread ( $\partial E_z/\partial z = 0$ ) cannot be achieved at any witness shape.

\*Work supported by RFBR grant 05-02-16775 and SB RAS Lavrent'ev grant for young researchers.

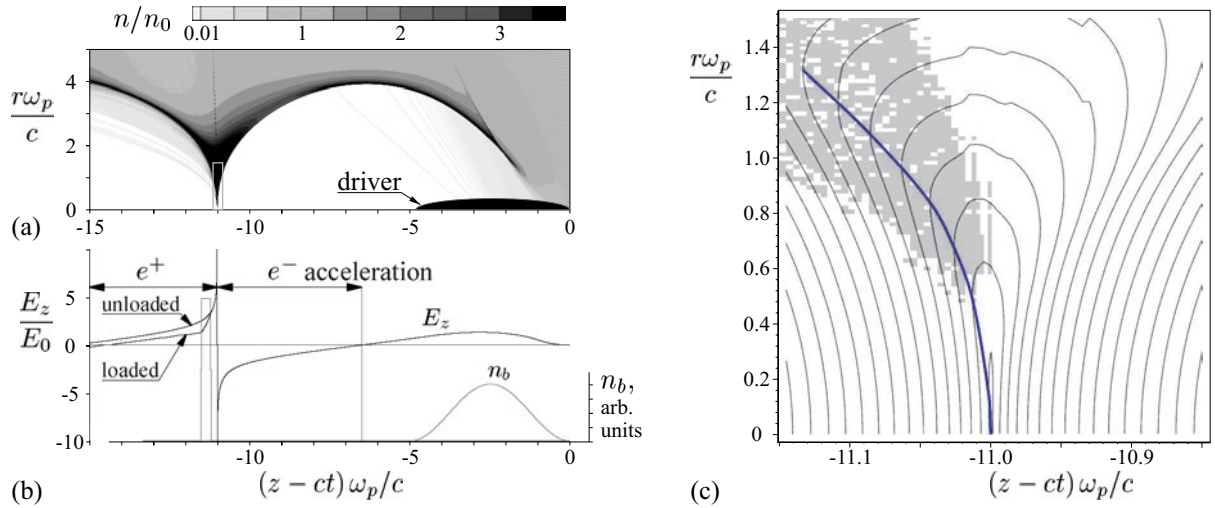


Figure 1: (a) Plasma electron density at  $\tilde{\Psi} = 70$ ; (b) on-axis electric field and driver density for this case; (c) isolines of the force potential  $\Phi$  near the end of the first bubble [in the area marked in (a) by the grey rectangle]. The thick line in (c) shows local minima of  $\Phi$  at  $z = \text{const}$ ; grey shading is the equilibrium location of test positrons initially injected near the axis. In (b), the field profile in the presence of a dense witness is also shown.

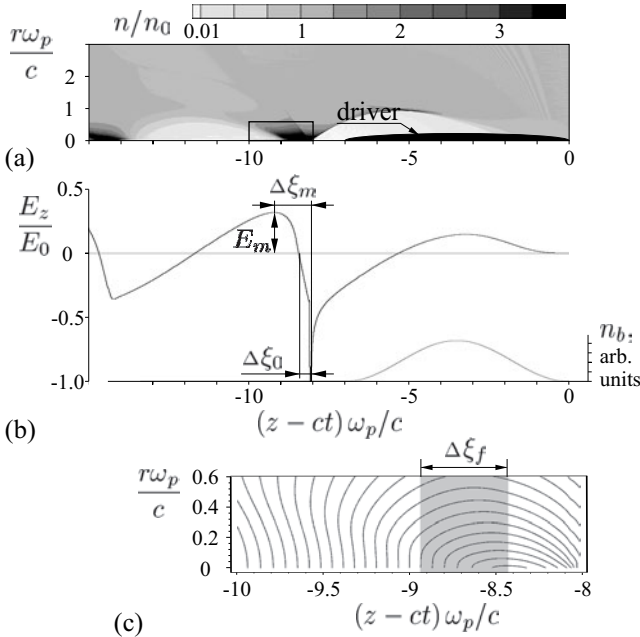


Figure 2: (a) Bubble shape, (b) electric field and beam density on the axis, and (c) shape of the potential well near the region of positron acceleration [rectangle in (a)] at  $\tilde{\Psi} \approx 0.3$ . The grey shading in (c) marks the area of both acceleration and favorable focusing.

For an electron witness, this problem does not appear since  $\partial|E_z|/\partial z < 0$  in the favorable region (Fig.1b). For positrons, the interval of  $\partial|E_z|/\partial z < 0$  at high  $\tilde{\Psi}$  is very short (Fig.1b), and presence of a density channel does not improve the situation. Thus, unlike electrons [5], for positrons the optimum performance is not associated with maximization of the peak driver current and wave energy.

As we see, the optimum place for accelerated positrons is located between the first and the second bubble. Let us

characterize the size and location of this region (acceleration basket) by the length of the favorable field slope  $\Delta\xi_m$ , offset with respect to the first bubble  $\Delta\xi_0$ , and length of the favorable focusing interval  $\Delta\xi_f$  (Fig.2). The measure of the field strength is the maximum field  $E_m$  (Fig.2b).

At first glance it would seem that the above quantities depend on many driver parameters like charge, radius, length, and shape. In reality, once the bubble is formed, the wave characteristics over a wide range of driver parameters are well determined by the single number, namely, the energy flux (1) behind of the driver. The flux dependence of the acceleration basket parameters are shown in Figure 3. Here the dots corresponds to Gaussian-shape drivers of various rms-length  $\sigma_z$  ( $0.02 \leq \sigma_z\omega_p/c < 3$ ) and peak current  $I_m$  ( $0.1 \leq I_m e/(mc^3) \leq 1.2$ ). For longer beams ( $\sigma_z\omega_p/c \gtrsim 3$ ), the beam tail touches the bubble end and the parameters of accelerating basket deviate from the above scaling. At moderate  $\tilde{\Psi}$ , the maximum field is well approximated as  $0.5 E_0 \sqrt{\tilde{\Psi}}$  (thin line in Fig. 3a). Two facts are seen from Fig. 3b,c. First,  $\Delta\xi_0 < \Delta\xi_f < \Delta\xi_m$ , that is, the acceleration basket begins when the field  $E_z$  becomes positive and ends as the focusing force changes its sign. Second, all sized exponentially decrease as the energy content of the wave grows. For example,  $\Delta\xi_m \approx e^{-\tilde{\Psi}/3} c/\omega_p$  (thin lines in Fig. 3b,c). Thus, for high  $\tilde{\Psi}$  it is extremely difficult to place accelerated positrons properly.

Once properties of the acceleration basket are determined by the dimensionless energy flux  $\tilde{\Psi}$ , it is natural to assume that the efficiency of positron acceleration is determined mainly by  $\tilde{\Psi}$  and by the field inside the witness  $E_w$ . We will define the efficiency as the ratio of the energy taken by the witness to the energy left by the driver in a unit length of the plasma. The maximum population of the positron beam is found in the same manner as it was done in [5] for electron beams. Namely, the witness current is

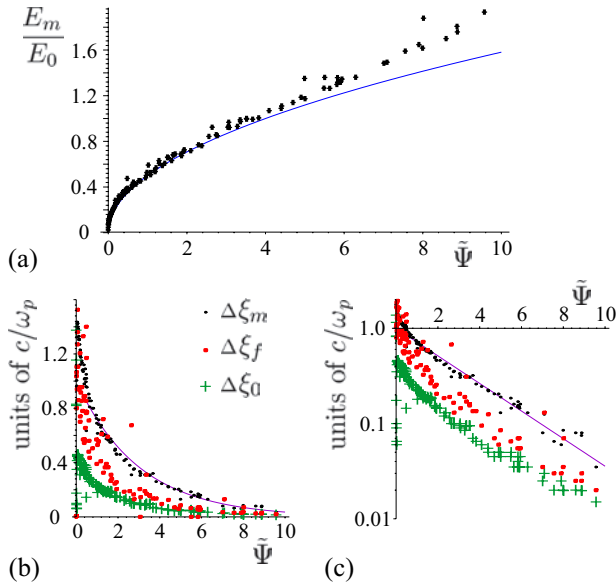


Figure 3: Maximum accelerating field  $E_m$  (a), and spatial dimensions of the acceleration basket in normal (b) and semi-logarithmic (c) scales as functions of  $\tilde{\Psi}$ .

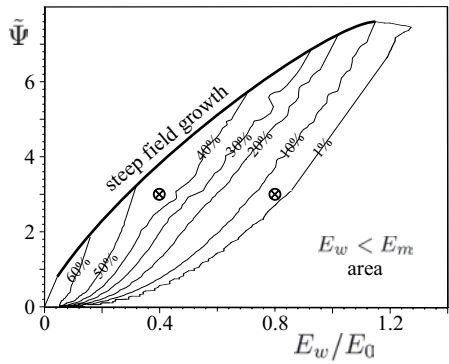


Figure 4: Isolines of the efficiency on the plane ( $E_w$ ,  $\tilde{\Psi}$ ).

adjusted slice-by-slice towards decreasing  $z$  in such a way as to have  $E_z = E_w = \text{const}$  on the axis. The witness ends when  $E_z$  gets smaller than  $E_w$  or the radial force near the axis changes its sign. The efficiency map thus obtained remains qualitatively the same as the driver shape or the witness radius change.

In Figure 4, the efficiency map is plotted for the Gaussian driver with  $\sigma_z = 1.4c/\omega_p$ ,  $\sigma_r = 0.1c/\omega_p$  and the same witness radius. The flux  $\tilde{\Psi}$  varies by changing the driver current. With a fine enough simulation grid, it is possible to construct a matched witness for very high  $\tilde{\Psi}$  and low  $E_w$  (top left corner of Fig. 4), but the location of this witness must be controlled with an exponentially high precision (see Fig. 3b,c). We exclude these unrealistic variants from consideration and show only the cases for which the distance between the witness and the point of  $E_z = 0$  is greater than  $0.01c/\omega_p$  (below the thick line in Fig. 4).

We see from Figure 4 that plasma-to-witness efficiencies of several tens percent are possible for positron beams. The ultimate efficiency is limited by the precision of witness shaping. At higher dimensionless accelerating rates,

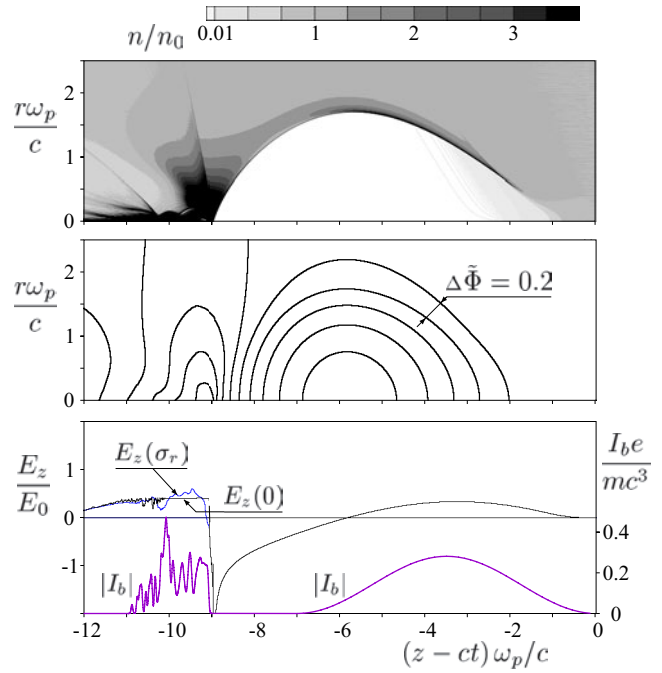


Figure 5: A matched driver-witness system at a moderate energy content of the wave ( $\tilde{\Psi} \approx 3$ ,  $E_w = 0.4E_0$ ): plasma electron density (top), isolines of the force potential  $\tilde{\Phi}$  (middle), longitudinal electric field  $E_z$  on the axis and at rms beam radius  $\sigma_r = 0.1c/\omega_p$ , and absolute value of beam current  $|I_b|$  (bottom).

higher energy content of the wave is required to stay within reasonable witness sizes.

An example of a matched driver-witness system is shown in Fig. 5 (parameters are marked in Fig. 4 by the crossed dot). We see from Fig. 5 that the positron beam is located in the region of high density of plasma electrons. As a consequence, the accelerating field varies across the beam even if on the axis it is exactly  $E_w$ . The resulting energy spread (of about several percent) cannot be minimized by reduction of the witness radius, since a narrow and dense positron beam attracts plasma electrons stronger and produces a higher inhomogeneity of  $E_z$ . The motion of plasma electrons in the presence of the witness is rather complicated, which determines a complicated shape of the matched witness. Plasma electrons attracted by the witness extend the potential well for positrons (see maps of  $\tilde{\Phi}$  in Fig. 5), so defocusing is not a limiting factor for a dense witness.

## REFERENCES

- [1] B. E. Blue, et al. Phys. Rev. Lett. **90** (2003) 214801.
- [2] S. Lee, et al., Phys. Rev. ST Accel. Beams **5** (2002) 011001.
- [3] S. Lee, et al., Phys. Rev. E **64** (2001) 045501.
- [4] J. B. Rosenzweig, et al., Phys. Rev. A **44** (1991) 6189.
- [5] K. V. Lotov, Phys. Plasmas **12** (2005) 053105.
- [6] K. V. Lotov, Phys. Rev. ST Accel. Beams **6** (2003) 061301.
- [7] K. V. Lotov, Phys. Plasmas **5** (1998) 785.
- [8] K. V. Lotov, Phys. Rev. E **69** (2004) 046405.